Cluster formation of nanoparticles in an optical trap studied by fluorescence correlation spectroscopy

Chie Hosokawa, Hiroyuki Yoshikawa,* and Hiroshi Masuhara†
Department of Applied Physics and Handai Frontier Research Center, Osaka University, 2-1 Yamadaoka, Suita, Osaka 565-0871, Japan
(Received 20 April 2005; revised manuscript received 14 June 2005; published 29 August 2005)

We report *in situ* observation of cluster growth of nanoparticles confined in an optical trapping potential by means of fluorescence correlation spectroscopy. When an optical trapping force caused by a highly focused laser beam acts on nanoparticle suspensions, the number of nanoparticles increases and an assembly can be formed at the focal spot. The decay times of fluorescence autocorrelation curves were investigated as a function of the irradiation time of the laser beam and the laser power. In the initial stage of the optical assembling, the decay time increases with the irradiation time of the laser beam. On the other hand, in the later stage, a decrease of the decay time was observed. This behavior is explained successfully by using two models of Brownian motion under weak and strong optical trapping. It was revealed that trapping and clustering of nanoparticles proceed simultaneously and clusters confined in the focal spot make larger aggregates spontaneously.

DOI: 10.1103/PhysRevE.72.021408 PACS number(s): 82.70.Dd, 87.80.Cc, 83.10.Pp, 87.64.−t

I. INTRODUCTION

Optical trapping has made a critical contribution to trapping and manipulating microscopic objects in solutions [1–3]. A single focused laser beam has now become an established tool to hold a micrometer-sized particle in three dimensions. Applying optical trapping to nanoparticles and macromolecules, another interesting phenomenon is expected. When the particle size is smaller than the size of the trapping laser beam, a number of nanoparticles can be trapped and an assembly is formed at the focal spot. We have actually observed this "optical assembly" of several kinds of polymers [4–6] and nanoparticles [7,8]. Our goal is to control their size, shape, and properties by the incident power, irradiation time, wavelength, and spatial pattern of a focused laser beam and to demonstrate the high potential of the trapping force in preparing molecular assemblages. Therefore, we have investigated the minimum size of the trapped polymer [9], the relation to the hydrogen bonding network and the electrostatic repulsion force between polymers of the trapping force [5,10], and the possibility of molecular orientation controlled by a focused laser beam [11,12]. Moreover, the stability, fluctuation, and displacement from the focal point of the trapped objects have been measured to evaluate optical trapping [13–15].

Nevertheless, the dynamic process of optical assembly in real space has been rarely discussed due to the lack of mature methods for studying the diffusion properties both in the bulk solution and in the microscopic region. In earlier work, we investigated the temporal profile of the number of trapped nanoparticles as a function of the laser irradiation time by single-particle counting [16]. In 100-nm-sized particle suspensions, it was observed that particles were trapped one by one at the focal spot. On the other hand, in 40-nm-sized particle suspensions, clusters composed of a few particles were trapped and then escaped from the focal spot. From the experimental and numerically simulated results, it was revealed that a cluster of nanoparticles formed around the focal spot was selectively trapped in the case of relatively weak trapping. As the next stage of studies on optical assembly of nanoparticles, rearrangement and aggregation proceeding in the focal spot have to be investigated. In this paper, we examine it by means of fluorescence correlation spectroscopy.

Fluorescence correlation spectroscopy (FCS) is a powerful tool to study Brownian motion of single fluorescent molecules in solution [17–19]. The number of fluorescent molecules and the diffusion coefficient are obtained from the autocorrelation function (ACF) of the fluorescence intensity. The fluorescence fluctuation originates from dynamic processes characterized by the diffusion of single molecules and single nanoparticles which occurs in small volumes of the focusing laser beam. If the association of such molecules and nanoparticles proceeds in suspension, the characteristic diffusion property due to the association may be obtained by using the FCS method. Thus, FCS has found widespread application in fields including biological systems, intercellular protein dynamics, reaction kinetics, and so forth [20].

In this paper, we investigate the clustering of nanoparticles proceeding in the focal spot by FCS measurement. The decay times of autocorrelation curves were observed as a function of the laser irradiation time and the laser power. It was clearly found that clustering of nanoparticles proceeds concurrently with the optical trapping and the clusters formed spontaneously make larger aggregates in the focal spot.

II. EXPERIMENT

As sample suspension, polystyrene latex particles with fluorescent dye (Molecular Probes, FluoSpheres carboxylate-modified orange, diameter 200, 100 nm and nile red, 24 nm) were used. The surface of the particle is negatively charged

*Electronic address: yosikawa@ap.eng.osaka-u.ac.jp
†Electronic address: masuhara@ap.eng.osaka-u.ac.jp

by the carboxyl groups. These suspensions were prepared at 10^7-10^{13} particles/ml of the particle concentration by dilution of the stock solution, whose concentration is 2.6×10^{15} particles/ml. The particle concentration appearing henceforth is that of the bulk suspensions. Of course, the local concentration in the focal spot increases during optical trapping. A dynamic light scattering apparatus (Otsuka Electronics, DLS-70S) was used to confirm the average diameter of the spheres. The ζ potential of the 24-nm-sized particles was −49.3 mV, obtained with a ζ potential analyzer (Malvern Instruments, Zetasizer Nano-ZS). All experiments were performed at room temperature (293 K).

A 1064 nm fundamental beam from a cw neodymium-doped yttrium aluminum garnet (Nd^{3+}:YAG) laser (Spectron Laser System, SL-902T 1104) was used for optical trapping and two-photon excitation. The YAG laser was introduced into an optical microscope (Carl Zeiss, UMSP-50) and focused into the nanoparticle suspensions via a microscope objective (magnification ×100, numerical aperture 1.25). The sample solution was dropped into a 1-mm-depth well on a glass slide and covered by a cover slip of 0.17 mm thickness. Two-photon excitation fluorescence from nanoparticles trapped at the focal point was passed through a notch filter (Kaiser Optics) to remove the scattered excitation light and was detected by an avalanche photodiode (APD) (EG&G, SPCM-AQ). The output of the APD unit was connected to a correlator card (ALV, ALV-5000/EPP) and a counter board (National Instruments, PCI-6601) set in a PC. For FCS measurement, the fluorescence intensity was acquired for 2–30 s depending on the intensity. Autocorrelation functions were calculated by the correlator board and analyzed with IGOR PRO 4.0 (WaveMetrics) for analytical fitting to obtain the decay time.

III. RESULTS AND DISCUSSION

In general, a smaller particle is trapped with more difficulty in the focal spot, since the trapping potential (force) is proportional to the polarizability (particle volume). Figure 1(a) shows a temporal profile (binned in units of 50 ms) of the two-photon excitation fluorescence intensity from 24-nm-sized nanoparticle suspension at 2.6×10^9 particles/ml concentration. The spikelike signal is due to fluorescence from a trapped nanoparticle, which escapes from the well at short times. In other words, since the free Brownian motion of the nanoparticle is affected by the weak trapping potential, the nanoparticle should stay in the focal spot for a longer time than in other places. Therefore, Brownian motion under weak optical trapping needs a different description from that under strong trapping, and the two-photon FCS curve is described in the following expression [21–23]:

$$G_{\mathrm{diff}}(t)=\langle\delta I(t)\,\delta I(0)\rangle/\langle I(0)\rangle^2=1+g_{\mathrm{diff}}(0)(1+t/\tau_{\mathrm{BD}})^{-1}. \tag{1}$$

Here $g_{\mathrm{diff}}(0)\propto 1/N$, where N is the average number of particles in the effective focal volume. τ_{BD}, which is obtained by analytical fitting of a FCS curve to Eq. (1), is expressed as

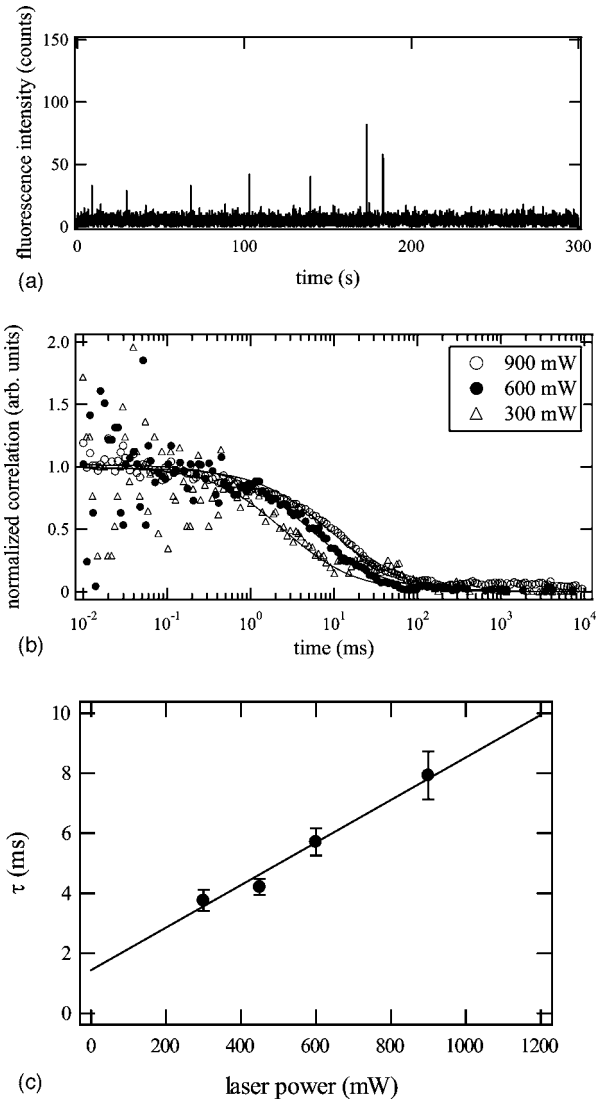

FIG. 1. (a) Temporal profile of two-photon excitation fluorescence intensity of 24-nm-sized particle suspensions (2.6×10^9 particles/ml) at 300 mW of laser power. (b) Typical normalized autocorrelation curves of the fluorescence fluctuations emitted from 24-nm-sized particle suspensions at the different laser power. Solid lines are results of least-squares fitting of Eq. (1). The noise observed at the early time is due to weak fluorescent signal. (c) The decay time τ of 24-nm-sized particle suspensions plotted as a function of the laser power. Solid line shows the theoretical values calculated from Eq. (2).

$$\tau_{\mathrm{BD}}=\tau_{\mathrm{D}}\exp(|U_{\mathrm{trap}}|/kT)\approx\tau_{\mathrm{D}}(1+|U_{\mathrm{trap}}|/kT) \tag{2}$$

where $\tau_{\mathrm{D}}=w_0^2/(8D)$ and w_0 is the beam waist, which is experimentally determined to be $w_0=0.45$ μm by the three-dimensional confocal fluorescence image of the 40-nm-sized nanoparticle [16]. D is the diffusion coefficient derived from the Stokes-Einstein equation, $D=kT/(6\pi\eta a)$, where η is the viscosity of solution and a is the radius of the particle. $|U_{\mathrm{trap}}|$ is the optical trapping potential, which is represented as $|U_{\mathrm{trap}}|=(n_2I_0\alpha)/(c\varepsilon_2)$, where I_0 is the laser intensity, α is the polarizability of the particle, c is the speed of the light, and

n_2 and ε_2 are the refractive index and the dielectric constant of the surrounding medium, respectively. τ_{BD} and τ_D correspond to average transit times of nanoparticles through a focal spot with and without the optical trapping potential, respectively. Equation (2) indicates that the transit time τ_D is biased by a small perturbation $|U_{trap}|/kT$ of the trapping potential. Here it should be noted that τ_{BD} increases as a function of the trapping potential $|U_{trap}|$, i.e., the laser power and the particle volume. Figures 1(b) and 1(c) show the autocorrelation curves at the different laser powers and the transit times τ_{BD} obtained by fitting the curves to Eq. (1) plotted as a function of the laser power, respectively. These are in good agreement with theoretical data (solid line) calculated from Eq. (2). For example, in the case of 24-nm-sized particle at the laser power of 300 mW, $\tau_D = 1.4$ ms, and $|U_{trap}| = 1.5kT$, the calculation gives $\tau_{BD} = 3.6$ ms and the averaged value obtained from experiments is 3.7 ms.

Here we briefly mention the temperature elevation induced by the trapping laser, which would influence data analysis. Some experimental results are reported that the temperature increases by less than 10 K/W [24–27] on focusing a subwatt YAG laser in water. In a recent example, Peterman *et al.* showed theoretically and experimentally that the temperature increase induced by trapping a 0.5 μm silica particle is ~8 K/W. We estimate that the autocorrelation functions are influenced by only a few percent by the temperature rise, so that temperature elevation caused by optical trapping can be neglected in our analyses henceforth.

Next, to evaluate our FCS analysis on the strong trapping potential ($|U_{trap}| > 10kT$), we present experimental results regarding 200-nm- and 100-nm-sized particles. As shown in our earlier work [16], a single particle at these sizes can be recognized by fluorescence. A single particle was trapped by focusing the laser beam in a dilute nanoparticle suspension and then the ACF of the two-photon excitation fluorescence was measured. As shown in Figs. 2(a) and 2(b), the autocorrelation curves strongly depend on the laser power and the particle size. Figure 2(c) shows the inverse ACF decay times obtained by exponential fitting of ACF curves as a function of the laser power. Since the trapping potential $|U_{trap}|$ is enough larger than kT($|U_{trap}| > 10kT$) under the present experimental conditions, the motion of the trapped nanoparticle is regarded as that in the harmonic potential generated by the focused laser beam. It has been obtained theoretically that Brownian motion in an optical harmonic potential shows the ACF decay time τ_{trap}, which is determined as follows [28,29]:

$$\tau_{trap} = \frac{6\pi\eta a}{|U_{trap}|/w_0^2} = 6\pi\eta a \frac{c\varepsilon_2 w_0^2}{n_2 I_0 \alpha}. \tag{3}$$

It is noteworthy that τ_{trap} is in inverse proportion to the trapping potential, i.e., the polarizability of the particle α and the laser power I_0. In addition, τ_{trap} is proportional to $1/a^2$, since the polarizability is proportional to a^3 in Eq. (3). This is opposite to that of weak trapping, in which τ_{BD} is proportional to I_0. Theoretical values calculated from Eq. (3) are also shown in Fig. 2(c) as solid lines. They are in good agreement with the experimental results, demonstrating that

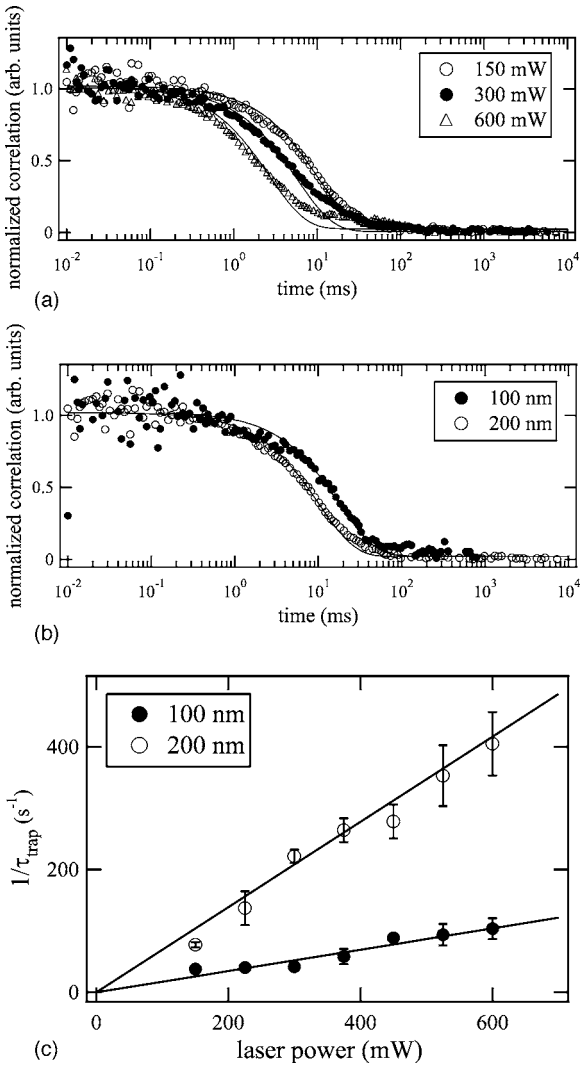

FIG. 2. (a) Laser power dependence in the 200-nm-sized particle suspensions and (b) particle size dependence at 150 mW of the laser power obtained from fluorescence autocorrelation curves of single trapped nanoparticle. Solid lines are results of exponential least-squares fitting. (c) The inverse decay times τ of ACFs versus the laser power. Solid line shows the theoretical values calculated from Eq. (3).

FCS analysis with our experimental setup gives quantitative data regarding the Brownian motion of trapped nanoparticles. Furthermore, we should point out that the ACF decay time τ of the strong trapping shows a different dependence on the trapping potential $|U_{trap}|$ from that of the weak trapping. If $|U_{trap}|$, i.e., particle size or laser power increases gradually during optical trapping, the τ should increase initially and then decrease. By use of these FCS analyses, hereafter we examine the optical assembly of 24-nm-sized nanoparticles.

Even in the case of weak trapping, optical assembly takes place under a high concentration of nanoparticles since another particle is trapped before the escape of one already trapped. Figure 3 shows temporal profiles of the fluorescence intensity of 24-nm-sized particles at 2.6×10^{13} particles/ml given at different laser powers. The fluorescence intensity in

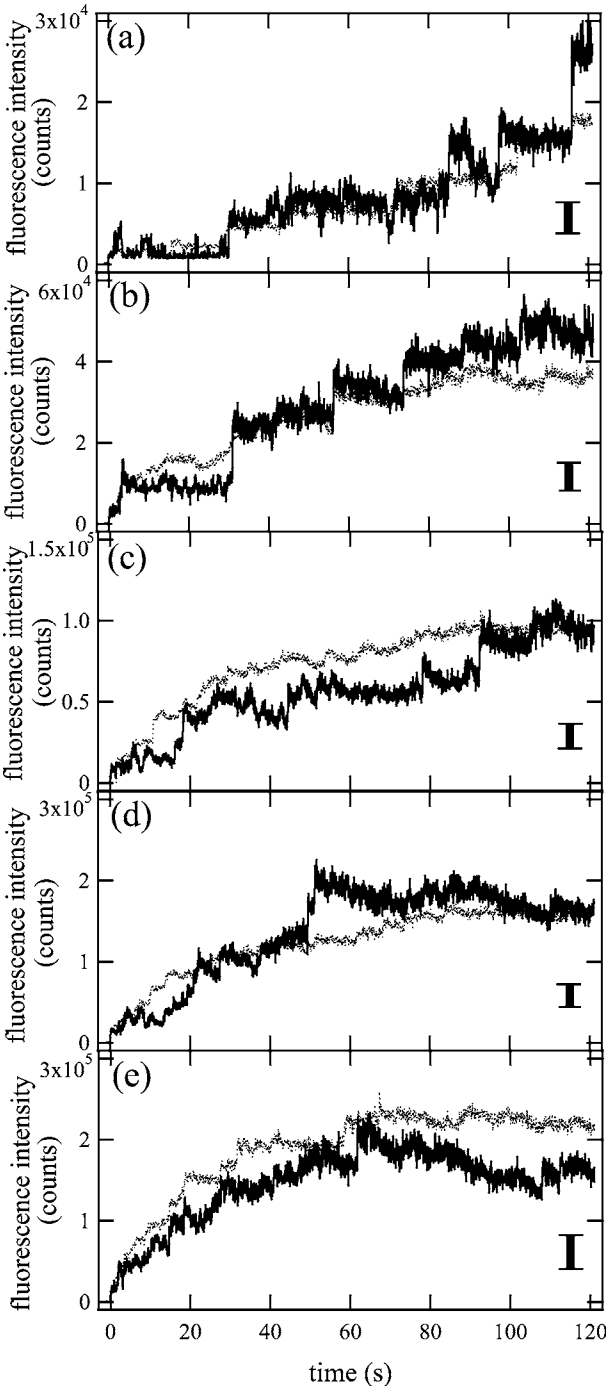

FIG. 3. Temporal profiles of two-photon excitation fluorescence intensity of 24-nm-sized particle suspensions (2.6×10^{13} particles/ml) measured with (a) 100, (b) 140, (c) 210, (d) 280, and (e) 350 mW of laser power. Solid lines are a representative result of a single measurement and dotted lines are averaged ones over seven measurements at each laser power, respectively. Vertical bars indicate fluorescence intensity corresponding to the particle number of 1.0×10^3 particles.

Fig. 3 reflects the number of nanoparticles in the trapping potential, where the depth of the potential is larger than kT. Its region was experimentally and numerically determined in earlier work to be ~1 μm in the focal plane and ~3 μm on the optical axis [16]. Before laser irradiation, the particle number in 1 μm^3 is estimated to be 26 particles/μm^3 at 2.6×10^{13} particles/ml of the concentration. On the other hand, it is demonstrated by the fluorescence intensity in Fig. 3 that the particle number reaches ~5000 particles at the focal spot at 120 s of the laser irradiation time, corresponding to 3.7 vol %. It is noted that the particle number in the trap exceeds that in the stock solution (2.6×10^{15} particles/ml). The fluorescence intensity (i.e., the number of nanoparticles) increases with the irradiation time and reaches a plateau value, indicating that 24-nm-sized particles are assembling in and filling up the focal spot. Figures 3(a)–3(e) clearly show that high power laser promotes growth of the assembly. The concentration (C_{trap}) in the trapping potential $|U_{\mathrm{trap}}|$ is described as $C_{\mathrm{trap}}=C_{\mathrm{bulk}}\exp(|U_{\mathrm{trap}}|/kT)$, where C_{bulk} is the concentration of the bulk suspension. In the present case, the $|U_{\mathrm{trap}}|$ exerted on the individual nanoparticle is $(0.51-1.7)kT$ in Figs. 3(a)–3(e), that is, $C_{\mathrm{trap}}=(1.7-5.5)C_{\mathrm{bulk}}$. However, as described later, Fig. 3 shows that a number of nanoparticles more than this expectation is trapped, suggesting that aggregates, which are confined in the optical trap more strongly than individual nanoparticles, are formed during the optical assembly. Hereafter we discuss this aggregation process on the basis of FCS analyses.

While the temporal profiles of fluorescence intensity were measured, FCS measurements were performed simultaneously. The ACF decay time τ is plotted as a function of the irradiation time of the laser beam in Fig. 4. This shows that the ACF decay time τ is clearly dependent on the laser irradiation time. In particular, at the low laser power of 100 mW [Fig. 4(a)], the decay time first increases during ~40 s and then decreases with increasing irradiation time. In addition, it is noted that the irradiation time when the decay time shows its maximum value becomes shorter (left shifted) with increase in the laser power. Figure 4 indicates that the Brownian motion dynamics of the optical assembly is strongly dependent on the laser irradiation time and the laser power.

We focus on Fig. 4(a) and discuss the optical assembling process of 24-nm-sized particles at low laser power. In Fig. 4(a), the ACF decay time obtained at the beginning of the optical assembly is $\tau=33\pm9.9$ ms, which is longer than the transit time $\tau_{\mathrm{BD}}=2.2$ ms calculated by Eq. (2). By substituting the ACF decay time $\tau=33$ ms into Eq. (2), it is estimated that the cluster consists of ~15 particles. This is in good agreement with the stepwise fluorescence increase in Fig. 3, showing that clusters of nanoparticles formed in the area surrounding the focal spot are trapped, as examined by single-particle counting in our earlier study [16]. Figure 3 demonstrates that the optical assembly proceeds by taking clusters into the focal spot. Such clusters are taken into the focal spot and the optical assembly proceeds.

Furthermore, the ACF decay time increases up to 40 s; however, the curve turns downhill after that. In this time region, the fluorescence intensity, i.e., the number of trapped nanoparticles, increases from beginning to end as shown in Fig. 3. On the other hand, the concentration in the focal spot is estimated to be 3.7 vol % at most, which is twice as large as that of the stock solution. This means that trapped particles (the original nanoparticles and aggregates) can move individually without any interaction. Therefore, the FCS data

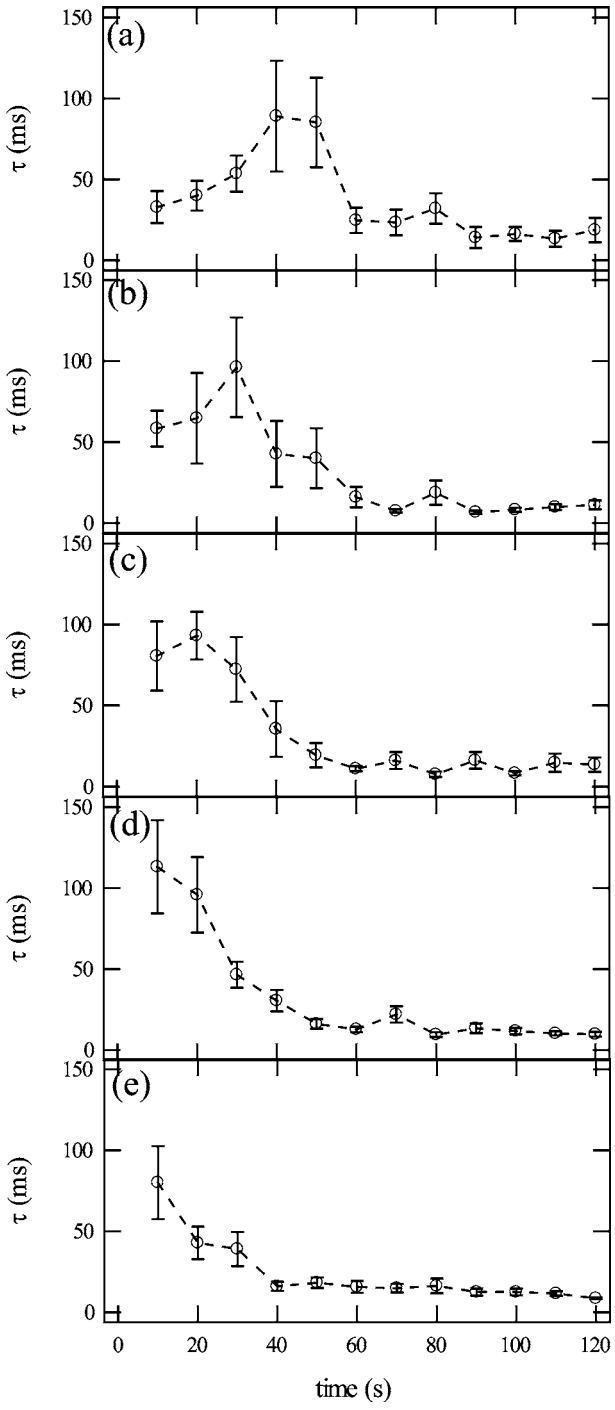

FIG. 4. Temporal profiles of the decay time τ of 24-nm-sized particle suspensions (2.6×10^{13} particles/ml) measured with (a) 100, (b) 140, (c) 210, (d) 280, and (e) 350 mW of laser power. The ACF is measured every 2–5 s during the irradiation of laser beam and the ACF decay time τ is obtained by the least-squares fitting of Eq. (1). Each figure (a)–(e) corresponds to Figs. 3(a)–3(e).

in Fig. 4 represent the Brownian motion of nanoparticles and clusters crossing and trapped in the focal spot as in Figs. 1 and 2. From these considerations, it was concluded that the change of ACF decay time in Fig. 4 can be attributed to aggregation of nanoparticles and clusters in the focal spot. Of course, the FCS data in Fig. 4 are contributed by many

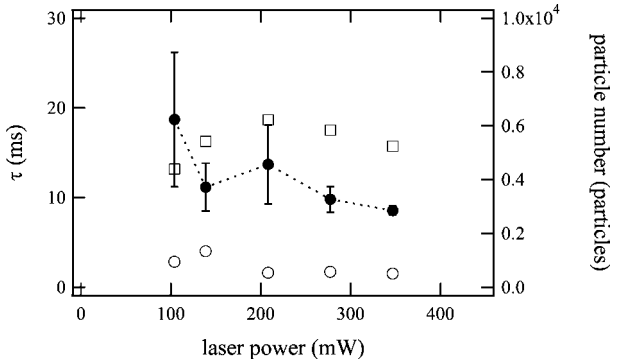

FIG. 5. Laser power dependence of the ACF decay time τ (closed circles) of 24-nm-sized particle suspensions at 120 s of the laser irradiation time. The particle number deduced from the size of the aggregate (open circles) is estimated from the ACF decay time. From the fluorescence intensity, the particle number in a focal spot (open squares) is derived.

particles and clusters and show the mean value of their distribution. In the earlier part of the assembly up to 40 s, the aggregation of the trapped clusters occurs, resulting in the increase of the trapping potential $|U_{\mathrm{trap}}|$ and ACF decay time τ according to Eq. (2). As shown in Fig. 3(a), the number of trapped nanoparticles is increasing in this time region, so that trapping and aggregation are proceeding simultaneously and the optical trapping force is getting strong due to the growth of the cluster volume. Therefore, in the later part of the assembly, the intrinsic motion of nanoparticles changes from biased diffusion in the case of weak trapping to Brownian motion tightly confined in a harmonic potential. The decrease of the decay time after 40 s can be explained as the growth of the trapped clusters in the harmonic potential, since the ACF decay time is proportional to $1/a^2$ in Eq. (3). Accordingly, as the trapped clusters make larger aggregates, the decay time becomes shorter. The decay time reaches $\tau = 18 \pm 7.5$ ms at the end of the measurement as shown in Fig. 4(a). This corresponds to that of a 230-nm-sized aggregate, i.e., a compact aggregate of ~940 particles derived by Eq. (3). At the same time, the fluorescence intensity in Fig. 3 shows that ~4400 particles are trapped in the focal spot at least, so that at least a few large aggregates are confined in the strong trapping potential at the final stage of the assembly.

Figure 5 shows the ACF decay times at 120 s of laser irradiation time as a function of the laser power, indicating that the ACF decay times decrease with increase in the laser power. The particle number deduced from the size of the aggregate is calculated by means of substituting the decay time and the laser power in Eq. (3) and is plotted in Fig. 5 (indicated by open circles). This demonstrates that the size of the produced aggregates at the final stage of the assembly does not strongly depend on the laser power. This can be attributed to the depletion of particles around the focal spot.

The time when the ACF decay time shows a maximum value in Fig. 4 indicates the boundary between weak and strong optical trapping. Since the laser power is proportional to the trapping potential depth, a higher laser power makes the confinement of nanoparticles stronger. As the laser power

gets higher, the peak of the ACF decay time actually appears at shorter times as shown in Figs. 4(b)–4(e) due to strong confinement. Of course, a strong trapping potential makes the assembling rate (the number of trapped nanoparticles per unit time) increase. If the rapid aggregation of the trapped clusters is enhanced by optical trapping, the change of the decay time must become sharp with increase in the laser power. However, the rate of decrease of the decay time does not strongly depend on the laser power. It is noteworthy that optical trapping does not force the aggregation, but makes the local concentration of nanoparticles increase. As shown in Fig. 4, aggregation proceeds for several tens of seconds. On the other hand, the concentration in the focal spot is at most twice as high as that of the stock solution, which is stable for more than half a year, indicating that the colloidal stability has been degraded in the trapping potential. However, since the aggregation half-time $T_{1/2}=3\eta/(4kTN_0)$, where N_0 is the particle number in a unit volume, is 7.7 ms calculated by Smoluchowski theory at 2.6×10^{13}particles/ml concentration, the aggregation in the focal spot proceeding via a diffusion-limited process must be completed on the order of milliseconds. This means that the assembling process is not described as a diffusion-limited process and the trapped particles still have a repulsive potential, which is on the order of kT. Such particles are confined in a trapping potential whose energy is also comparable to the thermal energy kT. This soft confinement is a significant property of optical trapping, because nanoparticles trapped in the focal spot can rearrange the location of each particle. This means that nanoparticles can form a kind of self-assembly structure in the focal spot. A practical application of this optical assembly is the crystallization of macromolecules like proteins. By focusing the laser beam in the macromolecular solution, local increase in concentration and spontaneous nucleation are induced in the focal spot. This would produce a technique whereby the position and the number of nuclei can be controlled.

IV. CONCLUSIONS

We have investigated the clustering of colloidal nanoparticles in the focal spot by means of fluorescence correlation spectroscopy. The decay times of fluorescence autocorrelation curves were characterized by the irradiation time and the power of the laser beam. In the initial stage of the optical assembling process, the ACF decay time of the fluorescence intensity increases with irradiation time of the laser beam. This can be attributed to the clustering of nanoparticles as a result of the increase of the local concentration assisted by optical trapping. As the focal spot becomes saturated by trapped nanoparticles, the ACF decay time turns to a decrease, demonstrating that larger clusters formed in the focal spot are strongly confined. Furthermore, the peak of the ACF decay time appears at shorter time in the case of high laser power. However, the rate of decrease of the decay time does not strongly depend on the laser power, indicating that optical trapping increases the local particle density, but does not force aggregation. Recently nanoparticles have been considered as building blocks to fabricate functional nanostructures, so that self-assembly of nanoparticles is energetically studied. Our present study suggests that such assembled structures of nanoparticles can be produced at an intended position at the submicrometer level by optical trapping.

ACKNOWLEDGMENTS

The present work is partly supported by a Grant-in-Aid for Scientific Research (KAKENHI) (S) (Grant No. 14103006) from the Japan Society for the Promotion of Science (JSPS) and a Grant-in-Aid for Young Scientists (B) (Grant No. 14740384) from the Ministry of Education, Culture, Sports, Science and Technology of Japan. C.H. was supported by JSPS.

[1] A. Ashkin, IEEE J. Sel. Top. Quantum Electron. **6**, 841 (2000).
[2] D. G. Grier, Nature (London) **424**, 810 (2003).
[3] K. C. Neuman and S. M. Block, Rev. Sci. Instrum. **75**, 2787 (2004).
[4] J. Hotta, K. Sasaki, and H. Masuhara, J. Am. Chem. Soc. **118**, 11968 (1996).
[5] J. Hofkens, J. Hotta, K. Sasaki, H. Masuhara, and K. Iwai, Langmuir **13**, 414 (1997).
[6] P. Borowicz, J. Hotta, K. Sasaki, and H. Masuhara, J. Phys. Chem. B **101**, 5900 (1997).
[7] S. Ito, H. Yoshikawa, and H. Masuhara, Appl. Phys. Lett. **78**, 2566 (2001).
[8] H. Yoshikawa, T. Matsui, and H. Masuhara, Phys. Rev. E **70**, 061406 (2004).
[9] T. A. Smith, J. Hotta, K. Sasaki, H. Masuhara, and Y. Itoh, J. Phys. Chem. B **103**, 1660 (1999).
[10] J. Hotta, K. Sasaki, H. Masuhara, and Y. Morishima, J. Phys. Chem. B **102**, 7687 (1998).
[11] J. Hotta, K. Sasaki, and H. Masuhara, Appl. Phys. Lett. **71**, 2085 (1997).
[12] S. Masuo, H. Yoshikawa, H.-G. Nothofer, A. C. Grimsdale, U. Scherf, K. Müllen, and H. Masuhara, J. Phys. Chem. B **109**, 6917 (2005).
[13] K. Svoboda and S. M. Block, Annu. Rev. Biophys. Biomol. Struct. **23**, 247 (1994).
[14] F. Gittes and C. F. Schmidt, Methods Cell Biol. **55**, 129 (1998).
[15] K. Wada, K. Sasaki, and H. Masuhara, Appl. Phys. Lett. **76**, 2815 (2000).
[16] C. Hosokawa, H. Yoshikawa, and H. Masuhara, Phys. Rev. E **70**, 061410 (2004).
[17] D. Magde, E. Elson, and W. W. Webb, Phys. Rev. Lett. **29**, 705 (1972).
[18] M. Eigen and R. Rigler, Proc. Natl. Acad. Sci. U.S.A. **91**, 5740 (1994).

[19] W. W. Webb, Appl. Opt. **40**, 3969 (2001).
[20] R. Rigler and E. L. Elson, *Fluorescence Correlation Spectroscopy: Theory and Applications* (Springer, Berlin, 2001).
[21] M. A. Osborne, S. Balasubramanian, W. S. Furey, and D. Klenerman, J. Phys. Chem. B **102**, 3160 (1998).
[22] G. Chirico, F. Olivini, and S. Beretta, Appl. Spectrosc. **54**, 1084 (2000).
[23] K. M. Berland, P. T. C. So, and E. Gratton, Biophys. J. **68**, 694 (1995).
[24] Y. Liu, D. K. Cheng, G. J. Sonek, M. W. Berns, C. F. Chapman, and B. J. Tromberg, Biophys. J. **68**, 2137 (1995).
[25] Y. Liu, G. J. Sonek, M. W. Berns, and B. J. Tromberg, Biophys. J. **71**, 2158 (1996).
[26] S. Wurlitzer, C. Lautz, M. Liley, C. Duschl, and T. M. Fischer, J. Phys. Chem. B **105**, 182 (2001).
[27] E. J. G. Peterman, F. Gittes, and C. F. Schmidt, Biophys. J. **84**, 1308 (2003).
[28] R. Bar-Ziv, A. Meller, T. Tlusty, E. Moses, J. Stavans, and S. A. Safran, Phys. Rev. Lett. **78**, 154 (1997).
[29] N. B. Viana, R. T. S. Freire, and O. N. Mesquita, Phys. Rev. E **65**, 041921 (2002).